

Alma Mater Studiorum Università di Bologna
Archivio istituzionale della ricerca

A one-material cylindrical model to determine short- and long-term fluid-to-ground response factors of single U-tube borehole heat exchangers

This is the final peer-reviewed author's accepted manuscript (postprint) of the following publication:

Published Version:

Naldi C., Zanchini E. (2020). A one-material cylindrical model to determine short- and long-term fluid-to-ground response factors of single U-tube borehole heat exchangers. GEOTHERMICS, 86(July 2020), 1-10 [10.1016/j.geothermics.2020.101811].

Availability:

This version is available at: <https://hdl.handle.net/11585/752339> since: 2020-03-18

Published:

DOI: <http://doi.org/10.1016/j.geothermics.2020.101811>

Terms of use:

Some rights reserved. The terms and conditions for the reuse of this version of the manuscript are specified in the publishing policy. For all terms of use and more information see the publisher's website.

This item was downloaded from IRIS Università di Bologna (<https://cris.unibo.it/>).
When citing, please refer to the published version.

(Article begins on next page)

This is the final peer-reviewed accepted manuscript of:

C. Naldi, E. Zanchini, *A one-material cylindrical model to determine short- and long-term fluid-to-ground response factors of single U-tube borehole heat exchangers*, Geothermics 86, 2020, n° 101811

The final published version is available online at:

<https://doi.org/10.1016/j.geothermics.2020.101811>

Rights / License:

The terms and conditions for the reuse of this version of the manuscript are specified in the publishing policy. For all terms of use and more information see the publisher's website.

This item was downloaded from IRIS Università di Bologna (<https://cris.unibo.it/>)

When citing, please refer to the published version.

A one-material cylindrical model to determine short- and long-term fluid-to-ground response factors of single U-tube borehole heat exchangers

Claudia Naldi*, Enzo Zanchini

Department of Industrial Engineering (DIN), Alma Mater Studiorum University of Bologna, Viale Risorgimento 2, 40136 Bologna, Italy

*Corresponding author: claudia.naldi2@unibo.it

Abstract

A new cylindrical model is proposed, suitable to determine both the short-term and the long-term fluid-to-ground thermal response factor of a single U-tube borehole heat exchanger (BHE). In the model, a BHE is represented by an equivalent cylinder, with the same radius and heat capacity as the BHE. The cylinder is made of a homogeneous material and contains a heat-generating cylindrical surface with an equivalent radius, r_{eq} , optimized by repeated 2D finite-element simulations. The thermal resistance of the layer between r_{eq} and the BHE radius equals the BHE thermal resistance. A correlation yielding the optimized values of r_{eq} is provided.

Keywords

Borehole heat exchangers; Single U-tube; Fluid-to-ground response factor; Short-term; Long-term; Numerical method.

Nomenclature

b	Borehole buried depth	(m)
BHE	Borehole Heat Exchanger	
D_b	Borehole diameter	(mm)
GCHP	Ground-Coupled Heat Pump	
k	Thermal conductivity	(W m ⁻¹ K ⁻¹)
L	Borehole length	(m)
OMEC	One-Material Equivalent Cylinder	
q_l	Thermal power per unit length	(W m ⁻¹)
r	Radius, radial coordinate	(mm)

R_b	Borehole thermal resistance per unit length	(m K W ⁻¹)
s	Shank spacing	(mm)
T	Temperature	(°C)
$WRMSD$	Weighted Root Mean Square Deviation	(°C)
z	Vertical coordinate	

Greek symbols

(ρc)	Volumetric heat capacity	(MJ m ⁻³ K ⁻¹)
τ	Time	(h)

Superscripts

*	Reduced coordinate	
---	--------------------	--

Subscripts

b	Borehole heat exchanger	
eff	Effective	
eq	Equivalent	
f	Fluid	
g	Ground	
gt	Grout	
i	Inner, i -th	
m	Model	
o	Outer	
p	Pipe, polyethylene	
r	Real BHE	

1. Introduction

Ground-Coupled Heat Pumps (GCHPs) typically employ fields of vertical ground heat exchangers, often called Borehole Heat Exchangers (BHEs). In the design of a BHE field, each borehole is usually modeled as a line heat source or a cylindrical heat source, with infinite or finite length. These models yield the time evolution of the mean temperature of the borehole surface. The temperature of the circulating fluid is then obtained by adding the product between the linear heat flux and the linear steady-state thermal resistance of the BHE. Since the BHE internal geometry and heat capacity are ignored, these methods are not able to provide precise results in the short-term period, as demonstrated by Lamarche (2013).

Indeed, an accurate analysis of the short-term fluid-to-ground thermal response of a BHE can be relevant in the evaluation of the total BHE length. In fact, in the case of strongly variable building loads, the heat capacity of the BHE internal elements can dampen the rise, or fall, of the BHE-fluid temperature, and ignoring this effect can cause an over prediction of the total BHE length required. Moreover, the BHE short-term response is relevant in hourly simulations of heat pumps coupled to BHEs, because an incorrect evaluation of the temperature of the fluid leaving the BHEs causes an error in the calculation of the heat pump COP and, consequently, in the evaluation of the heat pump energy consumption. Finally, a precise analysis of the BHE short-term response is necessary in the estimation of the ground thermal properties and of the BHE thermal resistance through short-time TRTs (Javed et al., 2010).

Due to the complexity of the internal structure of a BHE, in recent years several researchers presented simplified methods to determine a BHE fluid-to-ground thermal response factor accurate for the short-time analysis. The methods can be either analytical or numerical and can be used only for short-term evaluations or for both short and long time periods. Several review papers have been presented on the topic, e.g. by Javed et al. (2009), Javed et al. (2010), and Li and Lai (2015).

In early studies (Austin, 1998; Yavuzturk and Spitler, 1999), transient finite volume models were proposed, in which the real internal structure of the BHE is modeled as pie sectors, subjected to a constant heat flux. Yavuzturk and Spitler (2001) provided a validation of their model (Yavuzturk and Spitler, 1999) through comparison with field data from an elementary school. The predicted and the actual temperature values of the fluid entering the heat pump were in good agreement.

Young (2004) employed the buried electrical cable model (Carslaw and Jaeger, 1959), where the cable core represents the BHE fluid and the cable sheath the BHE grout. He introduced a grout allocation factor to assign part of the grout thermal capacity to an equivalent-diameter pipe. Since the evaluation of this grout allocation factor is difficult, the practical implementation of the method is limited. De Carli et al. (2010) developed a model, called CaRM (Capacity Resistance Model), that

employs lumped capacities and thermal resistances, and can be used for single U-tube, double U-tube and coaxial BHEs. The temperature of the BHE fluid and of the ground can be evaluated at different depths and, for the ground, at different distances from the BHE axis, but the thermal capacity of the BHE is not considered in the model. Zarrella et al. (2011) improved the model by De Carli et al. (2010) to consider the thermal capacity of the filling material and that of the BHE fluid. Since only a limited portion of the ground can be modeled with a reasonable computational time, the model allows only a short-term analysis. Bauer et al. (2011) developed three two-dimensional thermal resistance and capacity models (TRCMs) that apply to either coaxial, or single U-tube, or double U-tube BHEs. The models consider the heat capacity of the grout and are validated with finite element simulations. Pasquier and Marcotte (2012) improved the TRCM for single U-tube BHEs by Bauer et al. (2011) by including the thermal capacities of the fluid and of the pipes. The model can be extended also to other BHE configurations, but neglects the finite length of the borehole. Ruiz-Calvo et al. (2015) proposed to separate the short-term and the long-term simulation to obtain lower computational times. The short-term model, based on the thermal network approach, simulates the BHE daily operation, and accounts for the heat transfer between the fluid, the borehole and the adjacent piece of ground. The long-term model evaluates the initial ground temperature of each day, by considering the thermal load of the previous day. The short-term model is developed starting from the work by Bauer et al. (2011) and introduces a vertical discretization of the BHE, by considering for each node a thermal network to simulate the radial heat transfer. The model is implemented in TRNSYS and validated against experimental measures.

The short-term thermal response of a BHE has been analyzed by other authors by employing line-source models. Li and Lai (2012) developed a 2D analytical model based on Jaeger's instantaneous line source solution for composite media (Jaeger, 1944). The tubes are modeled as infinite line sources releasing a uniform and constant power per unit length, placed at a given distance from the BHE axis. Different properties of soil and piles/grout are considered. The model is validated by comparison with the usual infinite line-source model, in the case of uniform thermal properties. The same authors (Li and Lai, 2013) presented also a simplified form of the solution, validated by comparison with the experiment by Beier et al. (2011). To analyze the short-term performance of the composite-medium line-source model by Li and Lai (2012, 2013), Yang and Li (2014) implemented a two-dimensional numerical model based on the finite volume method. Although the circulating fluid is not included in the computational domain, its heat capacity is taken into account through a time dependent boundary condition between fluid and pipes. The model is validated by comparison with experimental results (Beier et al., 2011). Wei et al. (2016) employed the composite-medium line-source model developed by Li and Lai (2012) to determine the analytical expression of the fluid-to-ground response factor as

mean temperature at an equivalent radius. The expression is simpler than those proposed by Li and Lai (2012, 2013). The model is validated by comparison with the experimental results of Beier et al. (2011). Zhang et al. (2016) developed a transient quasi-3D line source model, which introduces the concept of transient borehole thermal resistance and yields both the short-term and the long-term thermal response. The model considers the real BHE geometry and takes into account the thermal short circuiting between the tubes, but does not consider the heat capacity of the BHE fluid.

Several authors developed cylindrical models of U-tube BHEs where the real internal geometry is replaced by a set of cylindrical layers coaxial with the BHE.

Gu and O'Neal (1998) proposed a BHE model where the U-tube is replaced by a cylinder with an equivalent radius r_{eq} , expressed as a function of the outer radius of the polyethylene pipes and of the shank spacing. The expression is derived under steady-state conditions and is not very accurate during the initial part of the transient heat transfer process.

Shonder and Beck (1999) replaced the real U-tube with an equivalent cylinder. The latter is surrounded by a thin layer that accounts for the heat capacities of fluid and pipes, and by a grout layer with external radius equal to the BHE radius. The authors found a good agreement between their solution and experimental results.

Xu and Spitler (2006) developed a numerical model that approximates the real BHE structure with several concentric cylinders. The internal fluid annulus is surrounded by an equivalent convective-resistance layer, a tube layer, and a grout layer, surrounded by the ground. Expressions to determine the geometry and the thermal properties of each layer are provided. A heat flux boundary condition is applied at the inner surface of the fluid annulus. The model is validated against finite volume simulations.

Lamarche and Beauchamp (2007) modeled the BHE as a cylindrical layer with the same thermophysical properties as the grout, with external radius equal to that of the BHE, and internal radius r_{eq} , surrounded by infinite homogeneous ground. They employed the value of r_{eq} suggested by Sutton et al. (2002) and presented analytical solutions for the case of given uniform and time-constant heat flux and for the case of convective heat transfer with given value of the mean temperature of the BHE fluid. Since the model ignores the thermal capacity of the BHE fluid, it overestimates the fluid temperature rise for short times.

Bandyopadhyay et al. (2008a) proposed to employ the BHE model and the analytical solution developed by Blackwell (1954) to evaluate the fluid-to-ground thermal response of single U-tube BHEs. In the model, the BHE fluid is represented by a virtual solid cylinder, with the same heat capacity as the real fluid, that generates heat uniformly. The grout is assumed to have the same thermal properties as the ground.

Man et al. (2010) presented the analytical solutions for two BHE models. In both cases, the BHE is considered as a solid cylinder with the same thermal properties as the external ground, containing a cylindrical-surface source with negligible thickness, mass and heat capacity. This source represents the heat supplied by the fluid. The first model is 1-D axisymmetric, while the second is 2-D axisymmetric and takes into account the finite length of the BHE. The analytical solutions are validated by comparison with finite difference numerical computations.

Beier and Smith (2003) developed an equivalent cylinder model of the BHE, where the cylinder is composed of a grout annulus with external radius equal to the BHE radius, and internal radius such that the thermal resistance of the grout annulus is equal to the BHE thermal resistance. An analytical solution of the heat conduction problem is obtained by employing the Laplace transform method. Bandyopadhyay et al. (2008b) improved the model of Bandyopadhyay et al. (2008a) by considering different properties of grout and ground, and developed an analytical solution for the new model. The solution is obtained in the Laplace transformed domain and inverted through the Gaver-Stehfest numerical algorithm. The solution is validated by comparison with finite element simulations.

Javed and Claesson (2011) presented an analytical solution for the BHE equivalent-cylinder model employed by Bandyopadhyay et al. (2008b). The heat transfer problem is represented as a thermal network in the Laplace domain and the solution is given in the time domain in the form of an integral. The analytical model is validated through comparisons with a numerical model and with experimental results. Lamarche (2015) improved the model by Lamarche and Beauchamp (2007) and presented the analytical solution for the new model, that takes into account also the heat capacity of the BHE fluid. In the new model, the borehole is composed by a cylinder representing the fluid, with radius r_i , surrounded by a thin cylindrical layer representing the polyethylene pipes, with external radius r_{eq} , surrounded on turn by a cylindrical layer representing the grout, with external radius equal to that of the BHE. A given generation power per unit length is supplied to the fluid. The values of r_{eq} and r_i are adjusted to meet the real grout and pipe thermal resistances, and equivalent volumetric heat capacities are employed to meet the real heat capacities of grout, polyethylene and fluid. The author found a good agreement between his model and those proposed by Beier and Smith (2003) and by Javed and Claesson (2011).

Claesson and Javed (2011) coupled the short-term model presented in Javed and Claesson (2011) to a long-term model based on the finite line-source solution, reduced to a single integral. Up to a certain breaking time (100 h is recommended), the short-term response is employed. After that, the long-term response of the ground is used, shifted upwards to match the fluid temperature given by the short-term response at the breaking time.

Hu et al. (2014) developed a composite cylindrical model for BHEs and energy piles, starting from the composite line-source model by Bixel and van Pollen (1967). The model superimposes the effects of cylindrical heat sources and takes into account the heat capacity of the BHE fluid and of the grout. The model is validated by comparison with results from 3D numerical models. Gordon et al. (2017) extended the model by Hu et al. (2014) to coaxial boreholes and validated the extended model through experimental results.

Beier (2014) developed a U-tube BHE model that handles the fluid flow in each pipe separately and approximates the U-tube as two half pipes, and considers both the heat capacity of the fluid and that of the grout. The author presented an analytical solution for the vertical temperature distribution of the BHE circulating fluid, valid both for short-term and long-term periods. The explicit form of the solution is in the Laplace domain, and is inverted by using the Stehfest algorithm. The model is validated through comparison with a laboratory experiment (Beier et al., 2011).

In this paper, we are interested in BHE models suitable to determine a full-time-scale thermal response of a BHE field, avoiding the problem of matching short-term and long-term thermal responses. In order to obtain a full-time-scale thermal response of a BHE field, one needs to consider the whole field, because the thermal interference between BHEs becomes important in the long term (Cimmino and Bernier, 2014; Lamarche, 2017; Monzó et al., 2015; Naldi and Zanchini, 2019). Indeed, since the BHEs are fed in parallel with the same inlet temperature, and are not subjected to a uniform heat flux per unit length, the long-term thermal response of the field cannot be obtained by the superposition of the effects of the single BHEs (Naldi and Zanchini, 2019). A method suitable to obtain an accurate full-time-scale thermal response of a BHE field is to perform a CFD simulation of the whole field, by employing a BHE model valid also in the short term.

Therefore, we analyze the accuracy of some of the BHE models cited above, selected among those suitable for CFD simulations and valid both in the short and in the long term. Then, we present a new BHE model suitable for full-time-scale CFD simulations of BHE fields and applicable to any kind of BHE. The model represents the BHE as an equivalent cylinder made of a homogeneous material, having the same radius as the BHE, r_b , and containing a heat-generating cylindrical surface, with an equivalent radius r_{eq} , that reproduces the power supplied to the BHE fluid. The thermal conductivity and the volumetric heat capacity of the material of the equivalent cylinder are chosen so that the thermal resistance of the cylindrical annulus between r_{eq} and r_b is equal to the BHE thermal resistance, and the heat capacity per unit length of the equivalent cylinder is equal to that of the BHE. The optimal value of r_{eq} is determined by repeated 2D short-time finite element simulations. A correlation that gives directly the optimal value of r_{eq} is provided, for single U-tube BHEs with usual pipes and shank spacing between 70 mm and 110 mm.

2. Comparison of some existing models

Among the existing models that represent a U-tube BHE by an equivalent cylinder and can be employed for CFD simulations, we selected those proposed by Xu and Spitler (2006), Lamarche and Beauchamp (2007), and Lamarche (2015). The first was developed specifically for CFD simulations, while the others were conceived to provide analytical solutions. However, since we are interested here in models that can be applied for the CFD simulation of a BHE field, we will consider CFD applications of all these models.

The accuracy of these models is checked by comparison with the results of a simulation of the real BHE cross section. In this simulation, the fluid (water, in this paper) is modeled as a solid with a very high thermal conductivity, namely 1000 W/(m K) , in which a uniform generation term is imposed. The high thermal conductivity is employed to obtain a nearly uniform temperature distribution in the fluid region, in analogy with Xu and Spitler (2006) and Lamarche (2015). The thermal conductivity of the polyethylene pipes is replaced by an effective one, k_{peff} , to take into account the convective thermal resistance.

In the model by Xu and Spitler (2006), the equivalent cylinder is composed as follows: an equivalent grout layer with external radius equal to that of the BHE, r_b , and internal radius equal to $\sqrt{2}$ times the outer radius of the polyethylene pipes, r_{po} ; an equivalent tube layer with internal radius equal to the external one minus the actual U-tube wall thickness; a convection layer with internal radius equal to the external one minus 0.25 times the actual U-tube wall thickness; an equivalent fluid layer with extremely high thermal conductivity and internal radius equal to the external one minus 0.75 times the actual U-tube wall thickness. The equivalent grout and tube layers have the same thermal conductivity, determined so that the thermal resistance of their union is equal to the BHE thermal resistance, R_b , minus the convective one. The thermal conductivity of the convection layer is such that its thermal resistance equals the convective thermal resistance. The volumetric heat capacity of each layer is set to reproduce the heat capacity of the corresponding element of the BHE, except for the convective layer, that has a vanishing volumetric heat capacity. A uniform and constant heat flux is applied at the inner surface of the fluid.

In the model by Lamarche and Beauchamp (2007), the equivalent cylinder is composed of a grout layer with the same thermal properties as the BHE grout, having external radius r_b and internal radius chosen so that the thermal resistance of the layer equals R_b . A uniform and constant heat flux is applied at the inner surface of the grout.

In the model by Lamarche (2015), the equivalent cylinder is composed of: an equivalent grout layer with the thermal conductivity of the BHE grout, having external radius r_b and internal radius such that the thermal resistance of this layer is equal to that of the BHE grout; an equivalent tube layer

with thermal conductivity k_{peff} , having internal radius such that its thermal resistance equals that of the pair of tubes of the BHE, including the convective resistance; an equivalent fluid core with extremely high thermal conductivity, where a uniform generation term corresponding to the given power per unit length takes place. The volumetric heat capacity of each element of the model is chosen to reproduce the heat capacity of the corresponding BHE element.

The mean fluid temperature is evaluated as volume average in the fluid domain for the real BHE and for the model by Lamarche (2015), and as surface average on the inner boundary in the models by Xu and Spitler (2006) and by Lamarche and Beauchamp (2007).

Sketches of the real BHE and of the three models are illustrated in Fig. 1.

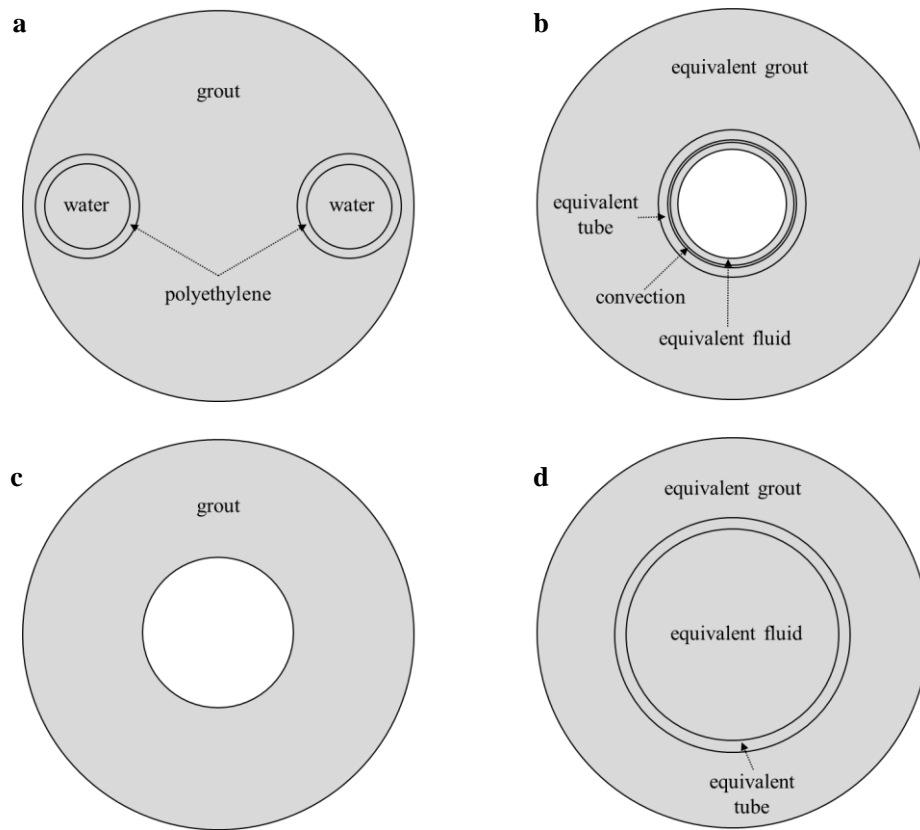


Fig. 1. Sketches of the cross section of the real BHE (a), and of the models by Xu and Spitler (2006) (b), Lamarche and Beauchamp (2007) (c), and Lamarche (2015) (d).

Since the models are built to reproduce the same thermal resistance as the BHE, they are all very accurate in the long term, where only the BHE thermal resistance is relevant. To compare the accuracy of these models, we consider the simulation of a single U-tube BHE subjected to a uniform and constant heat flux per unit length equal to 50 W/m, for a period of 100 hours from the operation start, and we concentrate the analysis mainly on the first hours of operation. The BHE selected has a diameter of 150 mm, a shank spacing of 100 mm, and tubes with external diameter 40 mm and internal

diameter 32.6 mm. The thermal conductivity of the grout is 1.6 W/(m K) and that of the ground is 1.8 W/(m K). The volumetric heat capacity of the grout is 2.25 MJ/(m³ K) and that of the ground is 3.00 MJ/(m³ K). The BHE fluid is water, with volume flow rate 14 liters per minute. The fluid properties are evaluated at 20 °C, through the NIST website <https://webbook.nist.gov/chemistry/fluid/>. The Reynolds number is 9082, and the convection coefficient, determined by the Churchill correlation at constant wall heat flux (Churchill, 1977), is 1472 W/(m² K). The BHE thermal resistance is evaluated by a steady-state 2D finite element simulation of the BHE cross section, implemented in COMSOL Multiphysics, that includes a portion of the surrounding ground, as recommended by Lamarche et al. (2010) and by Zanchini and Jahanbin (2018). The result is $R_b = 0.09466$ m K/W.

Transient 2D finite-element simulations are performed, through COMSOL Multiphysics, for the real BHE, for the model by Xu and Spitler, and for the numerical versions of the models by Lamarche and Beauchamp (2007) and by Lamarche (2015). A working time of 100 h is considered in each simulation, with steps equal to 0.05 in the logarithm of time in hours. A ground layer with external radius equal to 5 m and external adiabatic surface is considered around the BHE. The initial temperature is uniform and equal to the undisturbed ground temperature, T_g . A structured grid is built for each simulation, with about 6000 elements for the real BHE, about 2000 elements for the model by Xu and Spitler (2006) and for the numerical version of that by Lamarche and Beauchamp (2007), and about 3000 elements for the numerical version of the model by Lamarche (2015). Particulars of the grids employed in the simulations of the real BHE and of the numerical version of the model by Lamarche 2015 are shown in Fig. 2. The relative tolerance and the absolute tolerance are set equal to 0.0001 for each simulation.

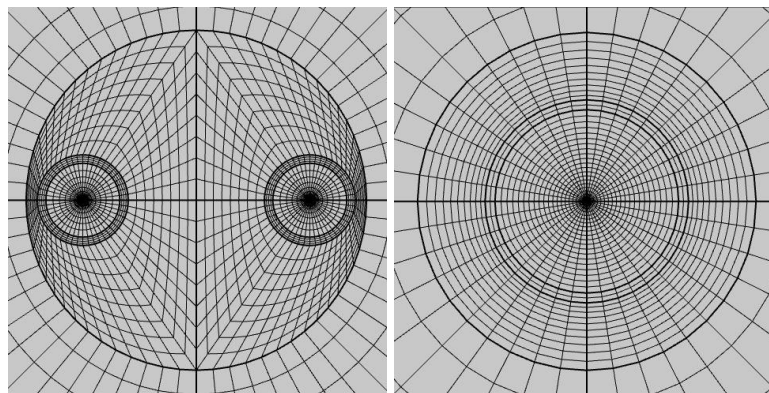


Fig. 2. Particulars of the meshes employed for the simulations of the real BHE (left) and of the numerical version of the model by Lamarche (2015) (right).

The independence of the results from the domain extension has been checked by replacing the adiabatic condition on the external boundary by the condition of uniform and constant temperature

$T = T_g$. Indeed, the adiabatic boundary condition yields an overestimation of the fluid temperature rise, $\theta = T_f - T_g$, while the isothermal condition yields an underestimation. Since identical values of θ have been obtained with the different boundary conditions, the independence of the results from the domain extension is ensured. The grid independence has been checked by repeating each simulation with a mesh regularly refined, with 4 times more elements. The values of θ obtained for each case with both meshes is illustrated in Table 1, for selected time instants. Since nearly identical results have been obtained by the refined grids, the mesh independence of the results is ensured.

Table 1 – Values of θ in °C at selected time instants for each case, with coarse and fine mesh.

	Time (h)				
	0.01	0.1	1	10	100
Real coarse	0.231	1.664	5.255	9.682	14.591
Real fine	0.231	1.664	5.255	9.682	14.591
Xu-Spitler coarse	0.217	1.420	5.036	9.681	14.620
Xu-Spitler fine	0.217	1.420	5.036	9.682	14.620
Lamarche-Beauchamp coarse	0.912	2.517	5.701	9.845	14.648
Lamarche-Beauchamp fine	0.912	2.517	5.701	9.845	14.648
Lamarche coarse	0.230	1.641	5.255	9.681	14.592
Lamarche fine	0.230	1.641	5.255	9.681	14.592

The temperature rise obtained in each simulation is plotted versus the logarithm of time in hours in Fig. 3. The figure shows that all the methods are precise in the long term, whereas the model by Lamarche (2015) is much more precise in the first hour. In the figure, the curve for the real BHE does not appear because it is covered by that for the model by Lamarche (2015). The numerical version of the model by Lamarche and Beauchamp (2007) overestimates the temperature rise in the short term because it does not consider the heat capacity of the fluid. On the other hand, the model by Xu and Spitler (2006) underestimates the temperature rise in the short term because it concentrates the heat capacity of the fluid in a narrow cylindrical layer with a rather small average radius, as is shown in Fig.1. The weighted root mean square deviation from the values of θ obtained by the real BHE simulation, $WRMSD$, is determined as

$$WRMSD = \sqrt{\frac{\sum_i \Delta \tau_i (\theta_m - \theta_r)_i^2}{\sum_i \Delta \tau_i}}, \quad (1)$$

where $(\theta_m - \theta_r)_i$ is the difference between the temperature rise determined through the model and that determined by the simulation of the real BHE, at the i -th time instant τ_i , and $\Delta\tau_i$ is half of the difference $\tau_{i+1} - \tau_{i-1}$.

The values of *WRMSD* obtained for the first hour are: 0.314 °C for the model by Xu and Spitler (2006), 0.604 °C for that by Lamarche and Beauchamp (2007), and 0.030 °C for that by Lamarche (2015). The corresponding values of *WRMSD* for the first 10 hours are: 0.115 °C, 0.309 °C and 0.010 °C, respectively.

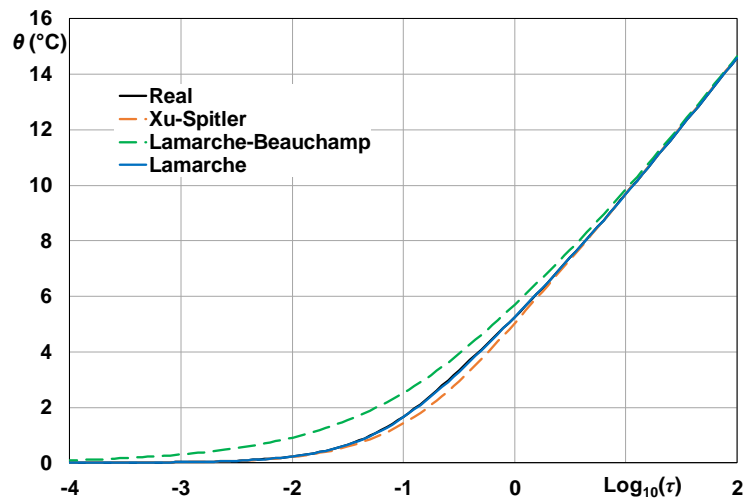


Fig. 3. Plots of θ versus the logarithm of time in hours for the real BHE and for the models.

3. The proposed model

In the new model, the BHE is represented by a One-Material Equivalent Cylinder, OMEC, with radius equal to the BHE radius, r_b . The cylinder contains a heat-generating cylindrical surface with an equivalent radius r_{eq} , whose value is optimized by repeated simulations, as explained later. A sketch of the OMEC cross section is shown in Fig. 4, left.

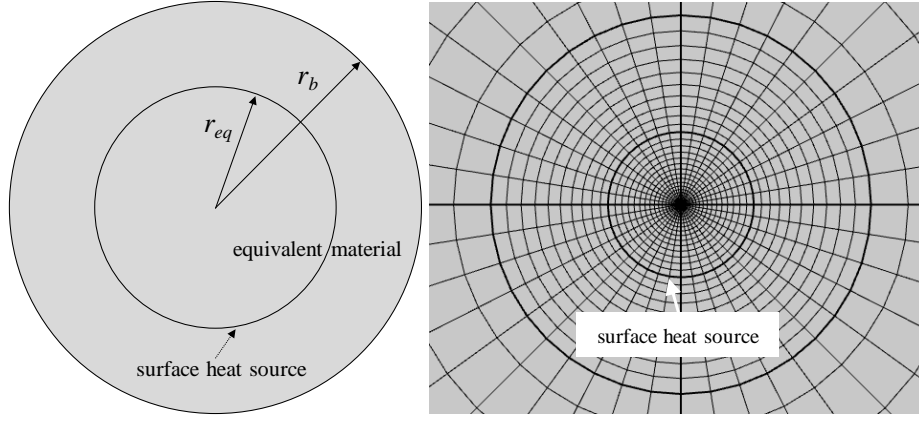


Fig. 4. Cross section of the OMEC (left) and particular of the structured grid employed (right).

The OMEC is made of an equivalent material, whose thermal properties are determined as follows. The heat capacity of the OMEC is the same as that of the BHE, and is the sum of the heat capacities of the BHE fluid, polyethylene and grout. As a consequence, the volumetric heat capacity of the OMEC, $(\rho c)_{eq}$, is given by

$$(\rho c)_{eq} = \frac{2\pi r_{pi}^2 (\rho c)_f + 2\pi (r_{po}^2 - r_{pi}^2) (\rho c)_p + \pi (r_b^2 - 2r_{po}^2) (\rho c)_{gt}}{\pi r_b^2}, \quad (2)$$

where r_{pi} and r_{po} are the inner radius and the outer radius of the polyethylene pipes, and $(\rho c)_f$, $(\rho c)_p$, $(\rho c)_{gt}$ are the volumetric heat capacities of the BHE fluid, polyethylene and grout, respectively. The value of the OMEC thermal conductivity, k_{eq} , is evaluated so that the thermal resistance per unit length of the cylindrical layer placed between r_{eq} and r_b is the same as that of the BHE, R_b :

$$k_{eq} = \frac{\ln\left(\frac{r_b}{r_{eq}}\right)}{2\pi R_b}. \quad (3)$$

For each case, the value of R_b is determined through a numerical steady-state simulation of the BHE cross section that includes a portion of the surrounding ground, and the convection coefficient is evaluated by the Churchill correlation with uniform wall heat flux.

The set of equations to be solved is

$$(\rho c)_{eq} \frac{\partial \theta(r, \tau)}{\partial \tau} = k_{eq} \nabla^2 \theta(r, \tau) \quad \text{for } 0 \leq r < r_b, \quad (4)$$

$$(\rho c)_g \frac{\partial \theta(r, \tau)}{\partial \tau} = k_g \nabla^2 \theta(r, \tau) \quad \text{for } r_b < r \leq r_g, \quad (5)$$

$$k_{eq} \frac{\partial \theta(r, \tau)}{\partial r} \Big|_{r=r_{eq}}^- - k_{eq} \frac{\partial \theta(r, \tau)}{\partial r} \Big|_{r=r_{eq}}^+ = \frac{q_l}{2\pi r_{eq}}, \quad (6)$$

$$-k_{eq} \frac{\partial \theta(r, \tau)}{\partial r} \Big|_{r=r_b}^- = -k_g \frac{\partial \theta(r, \tau)}{\partial r} \Big|_{r=r_b}^+, \quad (7)$$

$$\frac{\partial \theta(r, \tau)}{\partial r} \Big|_{r=r_g} = 0, \quad (8)$$

$$\theta(r, 0) = 0 \quad \text{for } 0 \leq r \leq r_g, \quad (9)$$

where r is the radial coordinate, τ is time, r_g is the radius of the computational domain, k_g and $(\rho c)_g$ are the thermal conductivity and the volumetric heat capacity of the ground, and q_l is the thermal power per unit length generated by the cylindrical surface of radius r_{eq} . Equation (6) implies that, at the internal boundary $r = r_{eq}$, the sum of the inward and outward heat fluxes per unit area is equal to the thermal power per unit area supplied by the heat-generating cylindrical surface. The value $q_l = 50$ W/m is employed.

To determine the optimal value of r_{eq} , finite-element simulations of transient heat conduction are performed with COMSOL Multiphysics, both for the cross section of the real BHE and for that of the OMEC, by employing trial values of r_{eq} , accurate up to 0.1 mm. Iterations are repeated until the *WRMSD* during the first hour reaches its minimum value. The simulations of the real BHE are performed as explained in Section 2. The simulations of the OMEC are performed with the same time steps, relative and absolute tolerance as those of the real BHE. The mean fluid temperature is evaluated as average on the surface with radius r_{eq} . A structured grid with about 3000 elements is employed. A particular of the grid for one of the cases studied is illustrated in Fig. 4, right.

4. Optimal values of the equivalent radius

The optimal values of the equivalent radius of the OMEC are determined for several single U-tube BHE configurations, and for different thermal properties of the ground and of the grout. Typical BHE diameters, namely $D_b = 140$ mm, 150 mm and 160 mm, are considered. Two values of the shank spacing, s , are considered for each BHE diameter: $s = 70$ mm and 90 mm for $D_b = 140$ mm; $s = 80$ mm and 100 mm for $D_b = 150$ mm; $s = 90$ mm and 110 mm for $D_b = 160$ mm. The inner radius r_{pi} and the outer radius r_{po} of the pipes are set equal to 16.3 mm and 20 mm, respectively. These are common values for single U-tube BHEs. The BHE fluid, that is water, has density 1000 kg/m³ and specific heat capacity 4.18 kJ/(kg K). The thermal conductivity and the volumetric heat capacity of polyethylene are set equal to 0.4 W/(m K) and 1.824 MJ/(m³ K). Three different values of the grout thermal conductivity, k_{gt} , are considered, namely 1 W/(m K), 1.6 W/(m K) and 2.2 W/(m K). Typical values of the grout volumetric heat capacity, $(\rho c)_{gt}$, are selected by referring to the experimental work by Kim et al. (2017): 1.50 MJ/(m³ K) and 2.25 MJ/(m³ K), for $k_{gt} = 1$ W/(m K); 2.25 MJ/(m³ K) and 3.00 MJ/(m³ K), for $k_{gt} = 1.6$ W/(m K) and $k_{gt} = 2.2$ W/(m K). Three different values of the ground

thermal conductivity, k_g , are considered, namely 1.4 W/(m K), 1.8 W/(m K) and 2.2 W/(m K). For each value of k_g , two different values of the ground volumetric heat capacity, $(\rho c)_g$, are selected, namely 1.50 MJ/(m³ K) and 2.25 MJ/(m³ K), for $k_{gt} = 1.4$ W/(m K); 2.25 MJ/(m³ K) and 3.00 MJ/(m³ K), for $k_g = 1.8$ W/(m K) and $k_g = 2.2$ W/(m K). These values of k_g and $(\rho c)_g$ are selected by referring to ASHRAE (2015), Chapter 34.

By combining the different values of the BHE geometric parameters with the different values of the grout and ground properties, 144 cases are selected and studied. For each case, the optimal value of r_{eq} obtained by repeated simulations is reported in Table 2.

Table 2

Optimal value of r_{eq} (mm) as a function of: k_{gt} and k_g (W/(m K)), $(\rho c)_{gt}$ and $(\rho c)_g$ (MJ/(m³ K)), D_b and s (mm).

k_{gt}	k_g	$(\rho c)_{gt}$	$(\rho c)_g$	$D_b=140$ $s=70$	$D_b=140$ $s=90$	$D_b=150$ $s=80$	$D_b=150$ $s=100$	$D_b=160$ $s=90$	$D_b=160$ $s=110$
1	1.4	1.50	1.50	34.2	31.4	33.5	30.6	32.7	29.9
			2.25	34.3	31.9	33.7	31.1	32.9	30.4
		2.25	1.50	28.2	25.3	27.5	24.5	26.7	23.8
			2.25	28.3	25.7	27.7	24.8	26.9	24.2
	1.8	1.50	2.25	34.3	31.9	33.6	31.1	32.9	30.3
			3.00	34.3	32.2	33.7	31.4	33.0	30.7
		2.25	2.25	28.3	25.7	27.6	24.8	26.8	24.1
			3.00	28.4	26.0	27.7	25.1	26.9	24.4
1.6	1.8	2.25	2.25	25.6	23.4	25.0	22.6	24.3	21.7
			3.00	25.6	23.7	25.0	22.7	24.4	22.1
		3.00	2.25	22.2	19.7	21.5	18.9	20.7	18.1
			3.00	22.3	20.0	21.6	19.2	20.9	18.4
	2.2	2.25	2.25	25.6	23.5	25.0	22.6	24.3	21.8
			3.00	25.7	23.8	25.0	22.7	24.4	22.1
		3.00	2.25	22.2	19.8	21.5	18.9	20.7	18.1
			3.00	22.3	20.1	21.6	19.2	20.9	18.4
2.2	1.8	2.25	2.25	23.9	21.7	23.1	20.8	22.3	20.0
			3.00	24.0	22.0	23.3	21.2	22.5	20.4
		3.00	2.25	20.4	18.1	19.6	17.2	18.9	16.4
			3.00	20.5	18.4	19.8	17.5	19.0	16.8
	2.2	2.25	2.25	23.9	21.8	23.2	20.9	22.4	20.1
			3.00	24.0	22.1	23.3	21.2	22.5	20.5
		3.00	2.25	20.5	18.2	19.7	17.3	18.9	16.5
			3.00	20.5	18.5	19.8	17.5	19.0	16.8

A correlation has been obtained, that gives directly the optimal value of the equivalent radius as a function of the BHE geometric parameters and of the thermal properties of the grout and of the ground:

$$r_{eq} = 0.0688569 - 0.0769444 D_b + 0.401042 D_b^2 - 0.0796181 s - 0.223958 s^2 - 0.00682856 k_{gt} + 0.0010395 k_{gt}^2 - 0.0166514 (\rho c)_{gt} + 0.00226852 (\rho c)_{gt}^2 + 0.0002875 (\rho c)_g, \quad (10)$$

where r_{eq} , D_b , and s are in m, k_{gt} is in W/(m K), $(\rho c)_{gt}$ and $(\rho c)_g$ are in MJ/(m³ K).

The correlation gives the optimal values of r_{eq} reported in Table 2 with a maximum discrepancy of ± 0.3 mm.

5. Validation of the simulation codes

The accuracy of the finite-element codes employed for the simulations of the OMEC has been checked by comparing the results obtained with those yielded by the analytical solution proposed by Man et al. (2010), for a BHE model that is a special case of the OMEC. Man et al. (2010) modeled the BHE as an infinite solid cylinder, with the same thermal properties as the ground, containing a heat-generating cylindrical surface of some radius r_0 . They presented an analytical expression of the fluid temperature rise, θ , as a function of the time, τ , and of the radial coordinate, r . For $r = r_0$, the solution is

$$\theta = -\frac{q_l}{4\pi^2 k_g} \int_0^\pi Ei \left\{ \frac{r_0^2 [\cos(\varphi) - 1]}{2\tau k_g / (\rho c)_g} \right\} d\varphi, \quad (11)$$

where q_l is the thermal power per unit length generated by the cylindrical surface and Ei is the exponential integral function.

In order to check the accuracy of our simulation codes, we consider a BHE with $D_b = 150$ mm and $s = 100$ mm, and with $q_l = 50$ W/m, $k_{gt} = k_g = 1.8$ W/(m K), $(\rho c)_{gt} = (\rho c)_g = 3.00$ MJ/(m³ K). The equivalent radius determined by Eq. (10) is $r_{eq} = 18.5$ mm. We perform in COMSOL Multiphysics a simulation of the OMEC with the method described in Section 3, by setting a power per unit area equal to $50/(2\pi r_{eq})$ W/m² on the OMEC heat-generating cylindrical surface. The comparison between the values of θ obtained by this simulation and those obtained by applying Eq. (11) with $r_0 = r_{eq}$ is illustrated in Fig. 5, where the values of θ are plotted versus the logarithm of time in hours, in the range $-3 \leq \log_{10}(\tau) \leq 2$. The figure evidences an excellent agreement of our simulation results with those obtained through the analytical expression by Man et al. (2010). The root mean square deviation of the values of θ obtained by the simulation from those obtained by Eq. (11) is 0.0014 °C.

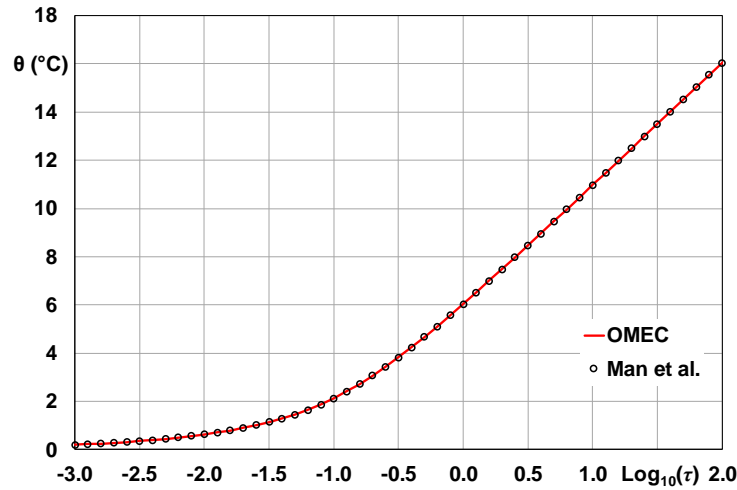


Fig. 5. Values of θ as a function of the logarithm of time in hours, by the OMEC and by Man et al. (2010).

6. Comparison between the OMEC and the model by Lamarche (2015)

In this section, we compare the accuracy of the OMEC with that of the numerical version of the cylindrical model by Lamarche (2015), that is the most accurate of those examined. We perform the comparison for the most common BHE diameter, namely $D_b = 150$ mm, and shank spacings $s = 80$ mm and $s = 100$ mm. The other parameters have the same values as in Section 2, i.e.: $k_{gt} = 1.6$ W/(m K), $k_g = 1.8$ W/(m K), $(\rho c)_{gt} = 2.25$ MJ/(m³ K), $(\rho c)_g = 3.00$ MJ/(m³ K), water volume flow rate 14 liters per minute. The values of r_{eq} determined by Eq. (10) are considered for the OMEC, namely 25.2 mm for $s = 80$ mm and 22.8 mm for $s = 100$ mm, so that the comparison takes into account the approximations due to the use of Eq. (10).

The comparison for $s = 80$ mm is illustrated in Fig. 6, where θ is plotted versus the logarithm of time in hours, for the real BHE, for the numerical version of the model by Lamarche (2015) and for the OMEC. Some differences between the results obtained by the three simulations can be seen only in the first hour. In the figure, the curve for the real BHE does not appear because it is covered by that for the model by Lamarche (2015) during the first 10 minutes, and by that for the OMEC after that time. The *WRMSD* of the values of θ from those obtained by the simulation of the real BHE is 0.072 °C for the numerical version of the model by Lamarche (2015) and 0.090 °C for the OMEC during the first hour, 0.043 °C for the model by Lamarche (2015) and 0.036 °C for the OMEC during the first 10 hours.

The corresponding plots for $s = 100$ mm are illustrated in Fig. 7. Again, some differences can be appreciated only in the first hour. The curve for the real case is covered by that for the numerical version of the model by Lamarche (2015) during the first 10 minutes and by the curves of both models after that time. The *WRMSD* from the values of θ obtained by the simulation of the real BHE is 0.030

°C for the model by Lamarche (2015) and 0.092 °C for the OMEC during the first hour, 0.010 °C for the model by Lamarche (2015) and 0.034 °C for the OMEC during the first 10 hours.

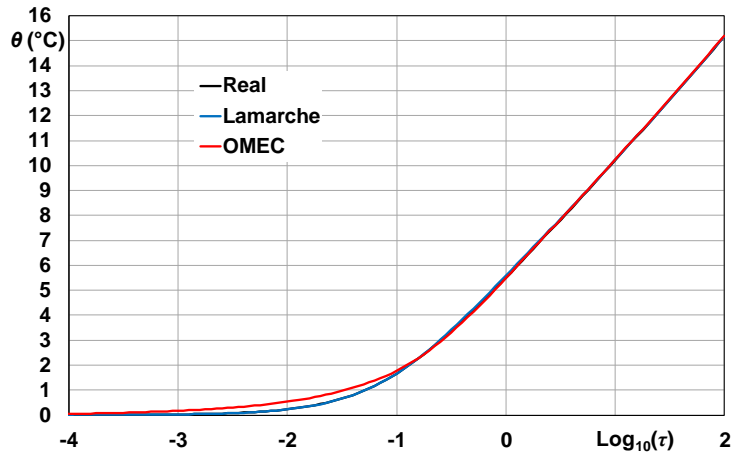


Fig. 6. Plots of θ versus the logarithm of time in hours for the real BHE, the numerical version of the model by Lamarche (2015), and the OMEC, BHE with $s = 80$ mm.

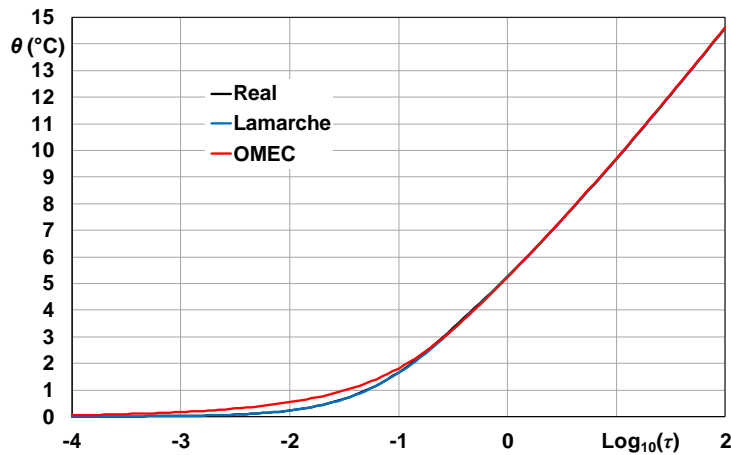


Fig. 7. Plots of θ versus the logarithm of time in hours for the real BHE, the numerical version of the model by Lamarche (2015), and the OMEC, BHE with $s = 100$ mm.

The comparison shows that both models are very accurate, with that by Lamarche (2015) slightly more accurate during the first 10 minutes, especially in the case with $s = 100$ mm, which is an upper bound of the shank spacing for $D_b = 150$ mm.

An advantage of the OMEC is its simpler implementation in numerical simulations of BHE fields, where several BHEs must be modeled. Another advantage is the lower number of dimensionless parameters that it requires for the parametric study of the dimensionless fluid-to-ground thermal

response factors of BHE fields with a given layout, such as square fields with a given number of BHEs.

7. Comparison between the 3D simulation of a 100 m long BHE and the simulation of the corresponding OMEC

In this section we show, by an example, the saving in grid complexity and computational time that can be obtained by replacing the 3D simulation of a real BHE with the 2D axis-symmetric simulation of the corresponding OMEC. Computations are performed by a PC with Intel Core i7-6700K 4.0 GHz, RAM 64 GB.

A BHE with $D_b = 150$ mm, $s = 100$ mm, length $L = 100$ m, buried depth $b = 2$ m, and water flow rate 14 liters per minute is considered, with the following properties of grout and ground: $k_{gt} = 1.6$ W/(m K), $k_g = 1.8$ W/(m K), $(\rho c)_{gt} = 2.25$ MJ/(m³ K), $(\rho c)_g = 3.00$ MJ/(m³ K). Simulations are performed for an operation time of 10000 h, with a uniform and constant power per unit length of 50 W/m supplied to the BHE fluid. The simulation domain is a cylinder with external radius 20 m and high 122 m, whose upper surface is the ground surface, kept at the undisturbed ground temperature. The bottom and the lateral surfaces of the domain are considered as adiabatic.

In order to compact the domain, the vertical coordinate z is replaced by the reduced coordinate $z^* = z/5$, and the thermal conductivity of each material in the vertical direction is replaced by the reduced conductivity $k^* = k/25$, according to the method used by Zanchini et al. (2010). Time steps in the logarithm of time in hours equal to 0.05 are employed from -5 to 4. The relative tolerance and the absolute tolerance are set equal to 0.0001.

Two 3D simulations of the real BHE are performed: the first with an unstructured mesh having 870013 tetrahedral elements, the second with a mesh obtained by a regular refinement of the first, having 6 960 104 tetrahedral elements. In both 3D simulations, the symmetry of the computational domain is exploited and only half of the domain is simulated. Then, two 2D axis-symmetric simulations of the OMEC are performed: the first with an unstructured mesh having 7705 triangular elements, the second with a mesh obtained by a regular refinement of the first, having 30820 triangular elements. Particulars of the grids employed in the second 3D simulation and in the first 2D axis-symmetric one are illustrated in Fig. 8. The computational time is about 50 minutes for the first 3D simulation and about 14 h and 11 minutes for the second; it is 9 seconds for the first 2D axis-symmetric simulation and 30 seconds for the latter.

The simulation results are illustrated in Fig. 9, where diagrams of θ versus the logarithm of time in hours are reported. The figure shows that the simulations of the OMEC yield a slight overestimation of θ during the first 6 minutes, as already revealed by the 2D simulations of a cross section, and

become very precise after that time. The zoom of the final part of the simulations shows a difference in θ of about $0.167\text{ }^{\circ}\text{C}$ between the 3D simulations, so that the refined grid can be considered as useful to achieve a very high accuracy. On the other hand, the difference in θ between the 2D axis-symmetric simulations is extremely small, namely $0.011\text{ }^{\circ}\text{C}$, so that the grid with 7705 elements is sufficient for a very high accuracy. We can conclude that the use of the OMEC allows a reduction of the computational time from 14 h 11 min to 9 seconds, without a loss of accuracy. For a comparison, the time evolution of θ for the same BHE is computed also by employing the numerical version of the model by Lamarche (2015). In order to obtain accurate results, a grid with about 50000 elements is required and the computation time is about 60 seconds. The computation time is higher than that required by the OMEC, but still acceptable. The main advantage of the OMEC model is the lower number of dimensionless parameters required to reproduce the real BHE. Indeed, 5 dimensionless parameters are sufficient: the dimensionless BHE thermal resistance, $R_b k_g$; the dimensionless BHE length, L/r_b ; the dimensionless BHE buried depth, b/r_b ; the dimensionless equivalent radius, r_{eq}/r_b ; the dimensionless equivalent volumetric heat capacity, $(\rho c)_{eq}/(\rho c)_g$. Many more dimensionless parameters are required by the Lamarche (2015) model. Therefore, the OMEC model is preferable for the parametric study of the dimensionless fluid-to-ground thermal response factors of a single BHE or of BHE fields, while the numerical version of the model by Lamarche (2015) is very useful for a validation of the results.

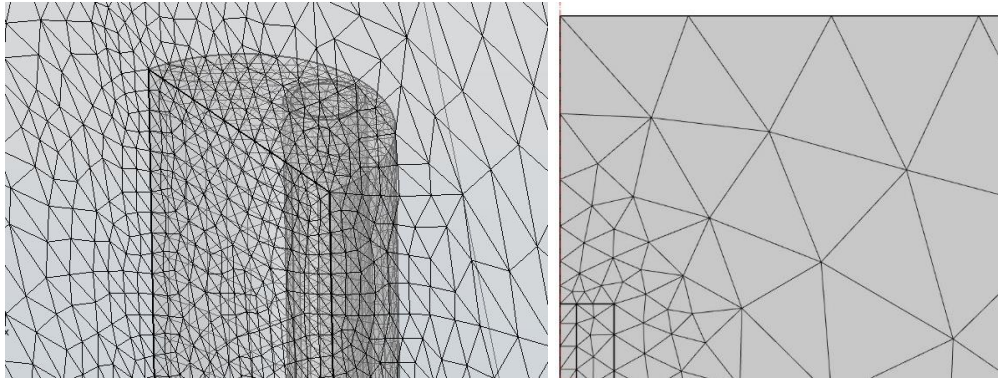


Fig. 8. Particulars of the grids at the BHE top, for the 3D simulation with the refined mesh (left) and for the 2D axis-symmetric simulation with the first mesh (right).

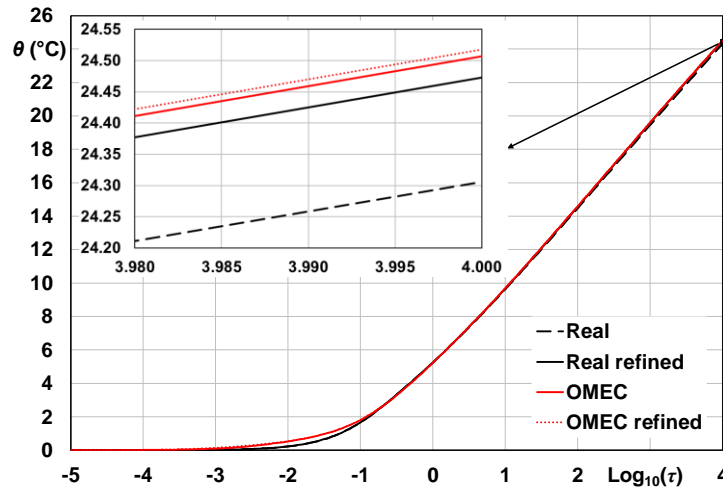


Fig. 9. Plots of θ versus the logarithm of time in hours for the 3D simulations of the BHE and for the 2D axis-symmetric simulations of the OMEC.

8. Conclusions

We have compared the accuracy of some existing cylindrical models of a single U-tube borehole heat exchanger (BHE), suitable for CFD simulations and valid both in the short and in the long term. The comparison has shown that the model by Lamarche (2015) is the most accurate.

Then, we have proposed a new model, where the BHE is represented by an equivalent cylinder made of a homogeneous material, having the same radius as the BHE and containing a heat-generating cylindrical surface with a suitable equivalent radius, r_{eq} . The thermal properties of the homogeneous material are such that the thermal resistance of the cylindrical annulus between r_{eq} and the BHE radius is equal to the BHE thermal resistance, and the heat capacity of the equivalent cylinder is equal to that of the BHE. By means of repeated finite-element simulations, we have determined the optimal value of r_{eq} for 144 cases, and we have provided a correlation that yields this value for single U-tube BHEs with usual pipes, BHE diameter between 140 and 160 mm, shank spacing between 70 and 110 mm, thermal conductivity between 1 and 2.2 W/(m K) for grout and between 1.4 and 2.2 W/(m K) for ground, and volumetric heat capacity between 1.50 and 3.00 MJ/(m³ K) for both grout and ground. The new model is slightly less precise than that by Lamarche (2015) for the first 10 minutes, and has the same accuracy after that time. Advantages of the new model are an easier implementation in numerical simulations of BHE fields and a lower number of parameters necessary to characterize a BHE field with a given shape and number of BHEs.

An application to the simulation of a finite-length BHE, with fluid replaced by a heat-generating solid, has shown that the new model allows reducing the computational time more than 5000 times, with respect to a 3D simulation of the real BHE with the same accuracy.

References

- ASHRAE, 2015. Geothermal energy, in: ASHRAE Handbook – Heating, Ventilating, and Air-Conditioning Applications. ASHRAE, Atlanta.
- Austin, W.A. III, 1998. Development of an in-situ system for measuring ground thermal properties. Master's thesis, Oklahoma State University, Stillwater, Oklahoma, USA.
- Bandyopadhyay, G., Gosnold, W., Mann, M., 2008b. Analytical and semi-analytical solutions for short-time transient response of ground heat exchangers. *Energy and Buildings* 40, 1816–1824.
- Bandyopadhyay, G., Kulkarni, M., Mann, M., 2008a. A new approach to modeling ground heat exchangers in the initial phase of heat flux build-up. *ASHRAE Transactions* 114 (2), 428–439.
- Bauer, D., Heidemann, W., Muller-Steinhagen, H., Diersch, H.-J.G., 2011. Thermal resistance and capacity models for borehole heat exchangers. *International Journal of Energy Research* 35, 312–320.
- Beier, R.A., 2014. Transient heat transfer in a U-tube borehole heat exchanger. *Applied Thermal Engineering* 62, 256–266.
- Beier, R.A., Smith, M.D., 2003. Minimum duration of in-situ tests on vertical boreholes. *ASHRAE Transactions* 109 (2), 475–486.
- Beier, R.A., Smith, M.D., Spitler, J.D., 2011. Reference data sets for vertical borehole ground heat exchanger models and thermal response test analysis. *Geothermics* 40, 79–85.
- Bixel, H.C., van Poolen, H.K., 1967. Pressure drawdown and buildup in the presence of radial discontinuities. *Society of Petroleum Engineers Journal* 7 (3), 301–309.
- Blackwell, J.H., 1954. A transient-flow method for determination of thermal constants of insulating materials in bulk, Part I – Theory. *Journal of Applied Physics* 25, 137–144.
- Carslaw, H.S., Jaeger, J.C., 1959. *Conduction of heat in solids*. Oxford University Press, Oxford.
- Churchill, S.W., 1977. Comprehensive correlating equations for heat, mass and momentum transfer in fully developed flow in smooth tubes. *Industrial & Engineering Chemistry Fundamentals* 16 (1), 109–116.
- Cimmino, M., Bernier, M., 2014. A semi-analytical method to generate g-functions for geothermal bore fields. *International Journal of Heat and Mass Transfer* 70, 641–650.
- Claesson, J., Javed, S., 2011. An analytical method to calculate borehole fluid temperatures for time-scales from minutes to decades. *ASHRAE Transactions* 117 (2), 279–288.

- De Carli, M., Tonon, M., Zarrella, A., Zecchin, R., 2010. A computational capacity resistance model (CaRM) for vertical ground-coupled heat exchangers. *Renewable Energy* 35, 1537–1550.
- Gordon, D., Bolisetti, T. Ting, D.S.-K., Reitsma, S., 2017. Short-term fluid temperature variations in either a coaxial or U-tube borehole heat exchanger. *Geothermics* 67, 29–39.
- Gu, Y., O’Neal, D.L., 1998. Development of an equivalent diameter expression for vertical U-tubes used in ground-coupled heat pumps. *ASHRAE Transactions* 104, 347–355.
- Hu, P., Zha, J., Lei, F., Zhu, N., Wu, T., 2014. A composite cylindrical model and its application in analysis of thermal response and performance for energy pile. *Energy and Buildings* 84, 324–332.
- Jaeger, J.C., 1944. Some problems involving line sources in conduction of heat. *The London, Edinburgh, and Dublin Philosophical Magazine and Journal of Science*, 35 (242), 169–179.
- Javed, S., Claesson, J., 2011. New analytical and numerical solutions for the short-term analysis of vertical ground heat exchangers. *ASHRAE Transactions* 117 (1), 3–12.
- Javed, S., Claesson, J., Fahlén, P., 2010. Analytical modelling of short-term response of ground heat exchangers in ground source heat pump systems. *Proceedings of the 10th REHVA World Congress, Clima 2010*. Antalya, Turkey, May 9–12.
- Javed, S., Fahlén, P., Claesson, J., 2009. Vertical ground heat exchangers: a review of heat flow models. *Proceedings of the 11th International Conference on Thermal Energy Storage – Effstock 2009*. Stockholm, Sweden, June 14–17.
- Kim, D., Kim, G., Kim, D., Baek, H., 2017. Experimental and numerical investigation of thermal properties of cement-based grouts used for vertical ground heat exchanger. *Renewable Energy* 112, 260–267.
- Lamarche, L., 2013. Short-term behavior of classical analytic solutions for the design of ground-source heat pumps. *Renewable Energy* 57, 171–180.
- Lamarche, L., 2015. Short-time analysis of vertical boreholes, new analytic solutions and choice of equivalent radius. *International Journal of Heat and Mass Transfer* 91, 800–807.
- Lamarche, L., 2017. g-function generation using a piecewise-linear profile applied to ground heat exchangers. *International Journal of Heat and Mass Transfer* 115, 354–360.
- Lamarche, L., Beauchamp, B., 2007. New solutions for the short-time analysis of geothermal vertical boreholes. *International Journal of Heat and Mass Transfer* 50, 1408–1419.
- Lamarche, L., Kajl, S., Beauchamp, B., 2010. A review of methods to evaluate borehole thermal resistances in geothermal heat-pump systems. *Geothermics* 39, 187–200.

- Li, M., Lai, A.C.K., 2012. New temperature response functions (G functions) for pile and borehole ground heat exchangers based on composite-medium line-source theory. *Energy* 38, 255–263.
- Li, M., Lai, A.C.K., 2013. Analytical model for short-time responses of ground heat exchangers with U-shaped tubes: Model development and validation. *Applied Energy* 104, 510–516.
- Li, M., Lai, A.C.K., 2015. Review of analytical models for heat transfer by vertical ground heat exchangers (GHEs): A perspective of time and space scales. *Applied Energy* 151, 178–191.
- Man, Y., Yang, H., Diao, N., Liu, J., Fang, Z., 2010. A new model and analytical solutions for borehole and pile ground heat exchangers. *International Journal of Heat and Mass Transfer* 53, 2593–2601.
- Monzó, P., Mogensen, P., Acuña, J., Ruiz-Calvo, F., Montagud, C., 2015. A novel numerical approach for imposing a temperature boundary condition at the borehole wall in borehole fields. *Geothermics* 56, 35–44.
- Naldi, C., Zanchini, E., 2019. A new numerical method to determine isothermal g-functions of borehole heat exchanger fields. *Geothermics* 77, 278–287.
- Pasquier, P., Marcotte, D., 2012. Short-term simulation of ground heat exchanger with an improved TRCM. *Renewable Energy* 46, 92–99.
- Ruiz-Calvo, F., De Rosa, M., Acuña, J., Corberán, J.M., Montagud, C., 2015. Experimental validation of a short-term Borehole-to-Ground (B2G) dynamic model. *Applied Energy* 140, 210–223.
- Shonder, J.A., Beck, J.V., 1999. Determining effective soil formation thermal properties from field data using a parameter estimation technique. *ASHRAE Transactions* 105 (1), 458–466.
- Sutton, M.G., Couvillion, R.J., Nutter, D.W., Davis R.K., 2002. An algorithm for approximating the performance of vertical bore heat exchangers installed in a stratified geological regime. *ASHRAE Transactions* 108 (2), 177–184.
- Wei, J., Wang, L., Jia, L., Zhu, K., Diao, N., 2016. A new analytical model for short-time response of vertical ground heat exchangers using equivalent diameter method. *Energy and Buildings* 119, 13–19.
- Xu, X., Spitler, J.D., 2006. Modeling of vertical ground loop heat exchangers with variable convective resistance and thermal mass of the fluid. *Proceedings of the 10th International Conference on Thermal Energy Storage, Ecstock 2006*. Pomona, New Jersey, May 31 – June 2.

- Yang, Y., Li, M., 2014. Short-time performance of composite-medium line-source model for predicting responses of ground heat exchangers with single U-shaped tube. *International Journal of Thermal Sciences* 82, 130–137.
- Yavuzturk, C., Spitler, J.D., 1999. A short time step response factor model for vertical ground loop heat exchangers. *ASHRAE Transactions* 105 (2), 475–485.
- Yavuzturk, C., Spitler, J.D., 2001. Field validation of a short time step model for vertical ground-loop heat exchangers. *ASHRAE Transactions* 107, 617–625.
- Young, T.R., 2004. Development, verification, and design analysis of the borehole fluid thermal mass model for approximating short term borehole thermal response. Master's thesis, Oklahoma State University, Stillwater, Oklahoma, USA.
- Zanchini, E., Jahanbin, A., 2018. Effects of the temperature distribution on the thermal resistance of double u-tube borehole heat exchangers. *Geothermics* 71, 46–54.
- Zanchini, E., Lazzari, S., Priarone, A., 2010. Improving the thermal performance of coaxial borehole heat exchangers. *Energy* 35, 657–666.
- Zarrella, A., Scarpa, M., De Carli, M., 2011. Short time step analysis of vertical ground-coupled heat exchangers: The approach of CaRM. *Renewable Energy* 36, 2357–2367.
- Zhang, L., Zhang, Q., Huang, G., 2016. A transient quasi-3D entire time scale line source model for the fluid and ground temperature prediction of vertical ground heat exchangers (GHEs). *Applied Energy* 170, 65–75.